Direct Numerical Simulation of a Round Jet into a Crossflow – Analysis and Required Resources

J.A. Denev[1], J. Fröhlich[2] and H. Bockhorn[1]

1 Institute for Technical Chemistry and Polymer Chemistry, University of Karlsruhe (TH)
Kaiserstraße 12, D-76128 Karlsruhe, Germany
{denev,bockhorn}@ict.uni-karlsruhe.de

2 Institute for Fluid Mechanics, Technical University of Dresden
George-Bähr Straße 3c, D-01062 Dresden, Germany
{jochen.froehlich}@tu-dresden.de

Abstract

Results from two Direct Numerical Simulations of a round jet in crossflow with velocity ratio of 3.3 are presented. The Reynolds number was 650 and 325. A passive scalar with Schmidt number of unity is introduced with the jet. The boundary conditions for both, jet and crossflow are laminar. This provides an unambiguous definition of the setup and favours its use as a test case. Transition of the jet was identified by an abrupt expansion of the average scalar field. The higher Reynolds number leads to a transition at 3.49 diameters downstream of the jet exit, the lower one - at 4.41 diameters. The higher Reynolds number flow exhibits smaller turbulent structures, but despite this and the different location of the transition, the trajectories of the two flows are close to each other.

The computational technique employed is a block-structured Finite-Volume method with local grid refinement at block boundaries implemented in the code LESOCC2. This allowed efficient distribution of cells so that 89% of them could be clustered in the vicinity of the jet exit and in the transition region. Issues of parallelization and efficiency are addressed in the text.

1 Introduction

The configuration of a jet issuing from a pipe into a crossflow (JICF) appears frequently in chemical, pharmaceutical, environmental and combustion engineering, to name but a few application areas. The complex vortical structures

of this flow and its good mixing capabilities make it a target of intense investigation for both experimental and numerical groups [7]. Previous work of the authors showed results from a Direct Numerical Simulations (DNS) of the jet in crossflow at Reynolds number $Re = 275$ (defined with the jet-diameter D and the crossflow velocity u_∞) and jet-to-crossflow velocity ratio $R = w_{jet}/u_\infty = 2.4$.

In the present study the results from two recent Direct Numerical Simulations (DNS) with velocity ratio $R = 3.3$ and Reynolds numbers $Re = 650$ and $Re = 325$ are compared. The influence of the Reynolds number on the vortex structures of the flow and its jet trajectory is presented in detail. As the jet in crossflow has a relatively complex structure, it is not trivial to generate a block-structured grid which is well-suited for this flow. As the efficient use of computer resources is specially important for studies with DNS, the present work focuses also on this issue.

2 Flow configuration

The flow configuration of a round transverse jet into a crossflow has been presented in detail in a previous work of the authors [1]. For brevity only the main parameters will be discussed here.

The pipe flow, from which the jet issues is laminar, as well as the crossflow. The laminar flow conditions allow to keep the boundary conditions of the investigation simple and unique (in contrast to, e.g. turbulence flow generators). However, during the interaction of the two streams transition to turbulence occurs and one of the targets of the present work is to investigate the characteristics of this transition and to establish its dependence on the Reynolds number in the range being studied. As the equations solved are in a non-dimensional form (with the jet diameter D and the crossflow velocity u_∞ set to unity in the computations), the Reynolds number is set directly as an input parameter for the computations.

In order to allow the simultaneous study of the mixing process and of chemical reactions in the configuration of the jet in crossflow, transport equations for passive and reactive scalars have been solved additionally to the incompressible Navier-Stokes equations. These equations govern the transport of non-reactive scalars and for them the Schmidt number has been varied and also the transport of reactive scalars in three simple chemical reactions and for them the influence of the Damkoehler number has been studied. Although according to the targets of the present investigation results only from one scalar transport equation are shown, the presence of a large set of partial differential equations for the remaining scalars should be beard in mind because it affects seriously the required computer resources for the investigation.

3 Numerical method

The simulation has been carried out with the collocated block-structured Finite Volume Code LESOCC2, developed at the Institute for Hydromechanics (IfH) of the University of Karlsruhe [5]. Second-order accurate schemes have been used for spatial discretization. The flow is treated as incompressible and a Poisson equation is solved for the pressure-correction equation.

No-slip boundary conditions have been applied at the walls of the channel crossflow with a boundary layer with a size larger than one pipe diameter. The simulated length of the pipe generating the jet is two diameters which has been found to be sufficient according to literature data and own preliminary simulations.

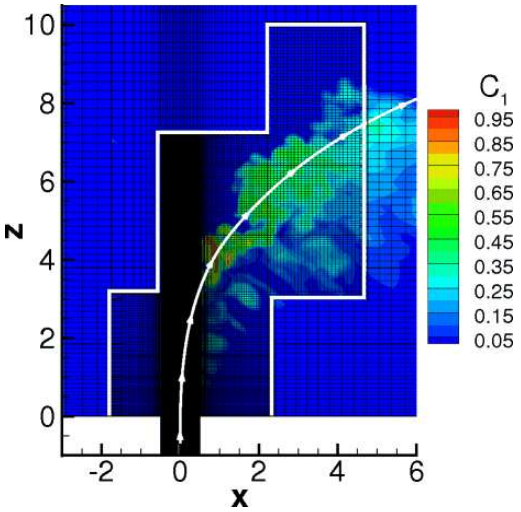

Fig. 1. The refined region of the grid in the midplane ($y = 0$), shown within the white boundaries. The local grid refinement factor is $3:1$ for all spatial directions of the numerical blocks near the jet-exit. The direction of the jet is upwards along the z-axes, the crossflow is along the x-axes (from left to right)

4 Local grid refinement for optimum distribution of grid nodes

The present investigation uses a block-structured curvilinear grid. Structured numerical grids have the drawback that finely resolved regions inevitably require fine mesh resolution throughout the whole computational domain. This

can lead to an unnecessary increase of the total number of control volumes. To overcome this drawback, the present study uses the local grid refinement technique, recently implemented in the code LESOCC2 [5]. The implementation allows two neighbour blocks to have a different number of control volumes at the two sides of their common boundary, see Fig. 1. Using this feature, the region near the jet exit is covered by small control volumes - in the present study 89% of the total number of control volumes are located there. The factor of refinement used is 3 : 1 for in all spatial directions.

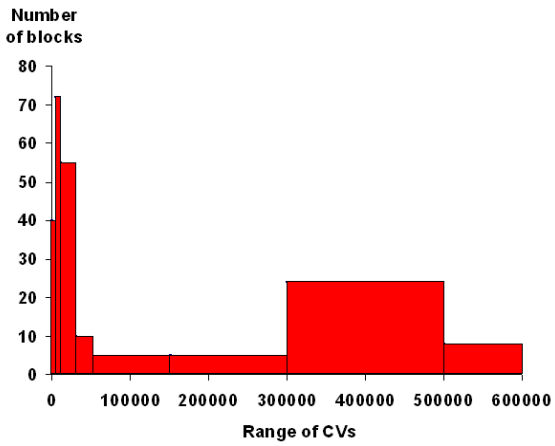

Fig. 2. Histogram: distribution of the number of control volumes for the 219 blocks

5 Parallel efficiency of the computations

The computations use a grid with 219 numerical blocks. At each Runge-Kutta step the computed variables are exchanged over the block boundaries. The algorithm requires that at each side of the block boundary two rows of additional halo cells are positioned. Those cells store the information for exchange by MPI (Message Passing Interface). Consequently, in a three-dimensional computation the percentage of halo cells can become large. For the present investigation the amount of the halo cells is 4 342 976, or 24% of the control volumes: this is the difference between the total number of computational nodes (22 320 832) and the number of control volumes (17 977 856).

The gridding process and the local grid refinement of the blocks near the jet outlet (Fig.1) lead to a disparity in the amount of control volumes per block. The histogram in Fig.2 shows the number of blocks for a certain range

of control volumes. A large number of small blocks exist, together with an increased number of large blocks.

The maximum number of processors to be used is generally limited by the size of the largest numerical block. For the present investigation the largest block (which has to be computed on a single processor) has 606 528 control volumes and there are 8 blocks of that size (cf. Fig. 2).

Fig. 3 shows the load balancing efficiency of the computations as a function of the number of processors for the present investigation. The graph is based on the statistics reported by the LESOCC2 code - after an optimization tool has been used for the distribution of the blocks over the processors. The load balancing efficiency does not take into account the computer hardware, but rather is a measure for the best achievable parallel efficiency. However, for the use of 31 processors, e.g., this information fully complies with the performance statistics of the HP XC4000 - both give 91% efficiency (i.e. 91% user time and 9% communication time). From the graph it is seen that the use of 31-32 processors presents an optimum for the present problem grid. Using more than 36 processors would decrease the parallel efficiency considerably, because of the restriction connected with the largest block size as mentioned above.

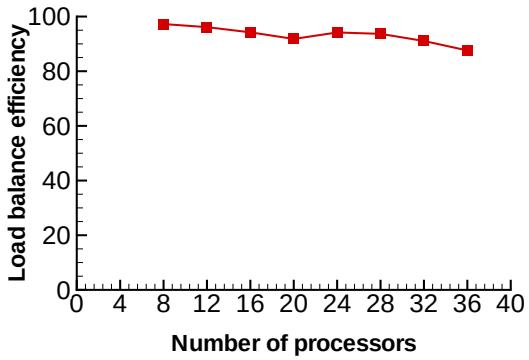

Fig. 3. Load balance efficiency for the present problem as a function of the number of processors

In order to increase the number of processors, a new blocking structure with more blocks and less control volumes per block would be required. This in turn would increase the number of halo cells and the communication time for MPI, thus decreasing the parallel efficiency of the computations. Some restrictions on the increase of processor number and control volume number currently apply due to the use of a commercial grid generator - ANSYS ICEM CFD which was employed in this project.

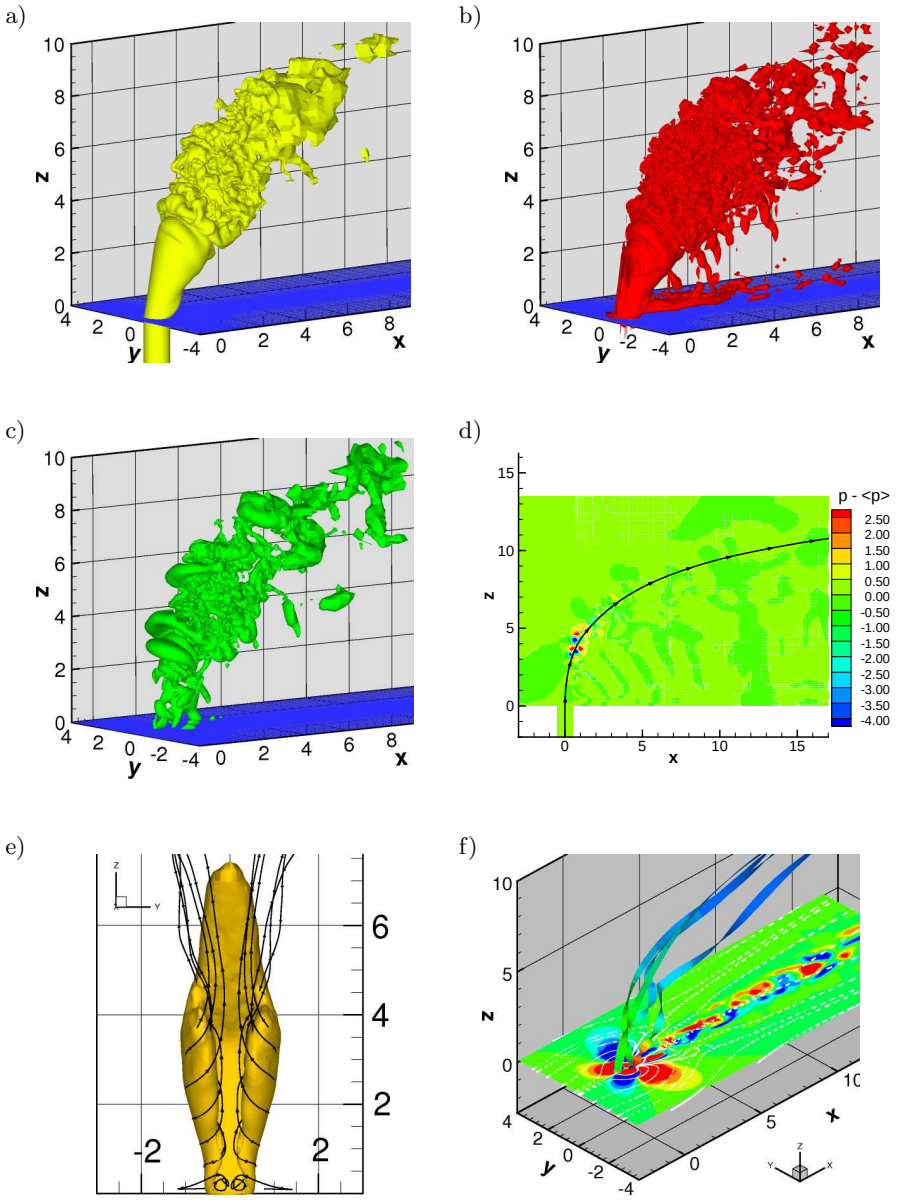

Fig. 4. Vortex structures of the jet in crossflow, simulation with $Re = 650$.
a) scalar concentration, $c_1 = 0.18$; b) the Q-criterion, $Q = 1.0$; c) pressure fluctuation, $p - \langle p \rangle = -0.1$; d) pressure fluctuation in the plane, $y = 0$; e) average scalar concentration, $\langle c_1 \rangle = 0.24$; f) $2D$ (white lines) and $3D$,(ribbons coloured by the concentration of the scalar) streamlines. The plane $z = 0.1$ is coloured by the z-vorticity.

6 Other numerical statistics from the computations

The computations have been carried out on the new HP XC4000 high performance computer at the Computer Centre of the University of Karlsruhe (TH). Thirty one processors (AMD Opteron, 2.6 GHz) have been used for the computations. In order to accumulate the required statistical data for the averaged variables, 105.7 dimensionless time units have been calculated (time units are based on the diameter of the jet-pipe and the velocity of the crossflow).

For the computations of these statistics the CPU-time (sum over all processors) was 35 708 hours for the run with $Re = 650$ (less than 2 months clock-time and practically no queuing time!). The lower Reynolds number case ($Re = 325$) required about 13.5% more CPU-time. This is due to the smaller time-step which is computed by the code based on stability criteria.

The CPU-time required per grid node and per time-step is 5.3E-05. This is based on the computation of the incompressible Navier-Stokes equations together with 3 equations for non-reacting passive scalars and 6 equations for reacting (but also passive in relation to the velocity field) scalars. The computation of all 9 scalar equations takes more than 2/3 of the CPU-time of the entire computation.

No restrictions connected with the RAM of the HP XC4000 have been noticed during the computations (required RAM per processor was 4Gb, the computations use practically below 25% of this).

Finally, during the test stage of the HP XC4000 its performance (still with the single rate (SDR) of the Infiniband 4X DDR interconnect) have been compared to the performance of HP XC6000. For the present computations the performance of the two machines has been practically identical. Also the comparison between the three FORTRAN 90 compilers available on the HP XC4000 (Intel, PGI and PathScale) showed the same performance (differences found were less than 1%).

7 Flow structures at Reynolds number 650

The jet in crossflow exhibits complex vortex structures, which have been the subject of research by many authors, e.g. ([3], [4], [6], [8]). Different variables are used here to allow a clear presentation of the corresponding vortices for the case with $Re = 650$ in Fig. 4. Figure 4a shows the instantaneous concentration field of scalar c_1 issuing from the pipe. The position of the transition as well as the formation of the first two ring-like vortices (the first one being in the zone prior to transition) is well identified on the figure.

Fig. 4b shows an isosurface of the Q-criterion [2]. Additional to the transition region, a clear picture of the upright vortices formed in the wake of the jet is obtained. In the boundary layer near the bottom wall two vortices directed downstream the crossflow are also observed.

Large vortices are characterized by regions of pressure minima. Fig. 4c shows the isosurface of the pressure fluctuation. The pressure fluctuation is defined as the averaged pressure, $\langle p \rangle$, subtracted from the instantaneous pressure, p, thus showing the locations of pressure minima. Three ring-like vortices are seen in the figure, with the third one being downstream of the transition region. Figure 4d shows the same variable $(p - \langle p \rangle)$ in the plane of symmetry $y = 0$ (the symmetry applies only to the averaged flow field!). Beside the two pressure minima, which coincide with the ring-like vortices in Fig. 4c, the locations of the upright vortices behind the jet are clearly seen (c.f. Fig. 4b).

All variables shown in Figures 4a, 4b, 4c and 4d were extracted for the same instant in time. They all show the clear presence of small-scale turbulent structures behind the region of transition together with the disorder and irregularity of the vortex structures typical for turbulent flows. The fifth figure (4e), unlike the previous four, shows an averaged isosurface of the scalar concentration together with some three-dimensional streamlines of the averaged velocity field. It allows the identification of the counter-rotating vortex pair (CVP) which is the most typical vortex structure of the jet in crossflow. In this Figure the jet is oriented towards the observer and the streamlines show the strong upward flow between the two vortices of the CVP. This upward flow contributes to the increased mixing capabilities of the transverse jet compared to a straight jet without crossflow. In the figure, the two downstream oriented vortices from Fig. 4b (close to the bottom wall) are visualized by two streamlines.

Finally, Fig. 4f shows some two- and three-dimensional streamlines of the averaged flow field from which again the complex vortex structure of the jet in crossflow can be deduced. The four "ribbons" originate from the pipe (positioned symmetrically close to the pipe walls at z=0). Two of them, starting from the "side" of the jet (coordinates of their origins being (0.;0.45;0.) and (0.;-0.45;0.)) are twisted by the vortices at the rear side of the jet and then taken upwards from the same upward flow shown in Fig. 4e. The vortices at the rear side of the jet are also seen on the $2d$ streamlines drawn in a horizontal plane at $z = 0.1$. The same plane is coloured by the vorticity component in direction of the z-axes, showing again the upright vortices from Figs. 4b and 4d.

8 The influence of the Reynolds number

In Fig. 5 the corresponding vortex structures for the case with two times lower Reynolds number ($Re = 325$) are presented and compared to the flow with $Re = 650$ (the dimensionless time of the accumulated statistics for this computation is 50). On this figure the same levels of the isosurfaces as in Fig. 4 are presented. Basically two important features can be seen from the comparison of the two figures. First, as it should be expected, the transition

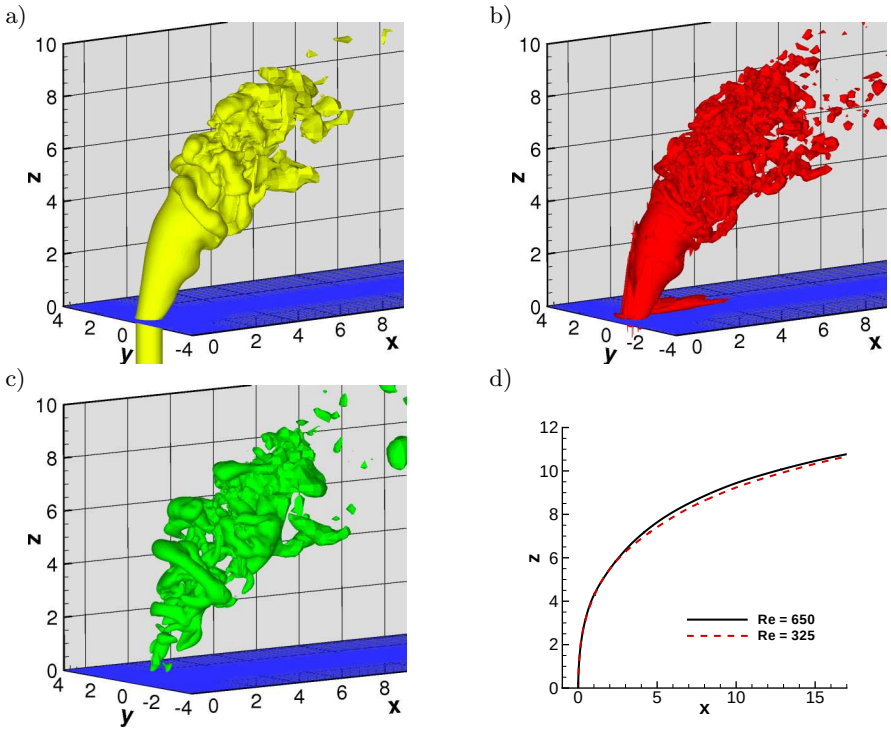

Fig. 5. Vortex structures for the case with $Re = 325$ and the central streamline (averaged velocity field) for the two DNS.
a) scalar concentration, $c_1 = 0.18$; b) the Q-criterion, $Q = 1.0$; c) pressure fluctuation, $p - \langle p \rangle = -0.1$; d) the central streamlines (0.;0.;0.) at $y = 0$.

region for the jet at $Re = 325$ is further downstream than that for $Re = 650$. Second, all the turbulent structures are clearly larger than the corresponding structures for $Re = 650$. Despite this, Fig. 5a,b,c shows that even in the case with $Re = 325$ the flow downstream of the transition region is irregular and turbulent.

Fig. 5d shows the influence of the Reynolds number on the two-dimensional streamline originating from the origin of the jet (coordinates (0.;0.;0.)). This definition of the jet streamline which sometimes also is called "streamline trajectory" ([9]) is computed from the averaged flowfield. The figure shows that the trajectory for the case $Re = 325$ is a bit lower than at $Re = 650$ and also that there is only little impact of the Reynolds number on the shape of the streamline trajectory. Here it should be noticed that the shape of the boundary layer at the channel walls has been exactly the same for the two flows studied in order to exclude the influence of all other parameters except the Reynolds number.

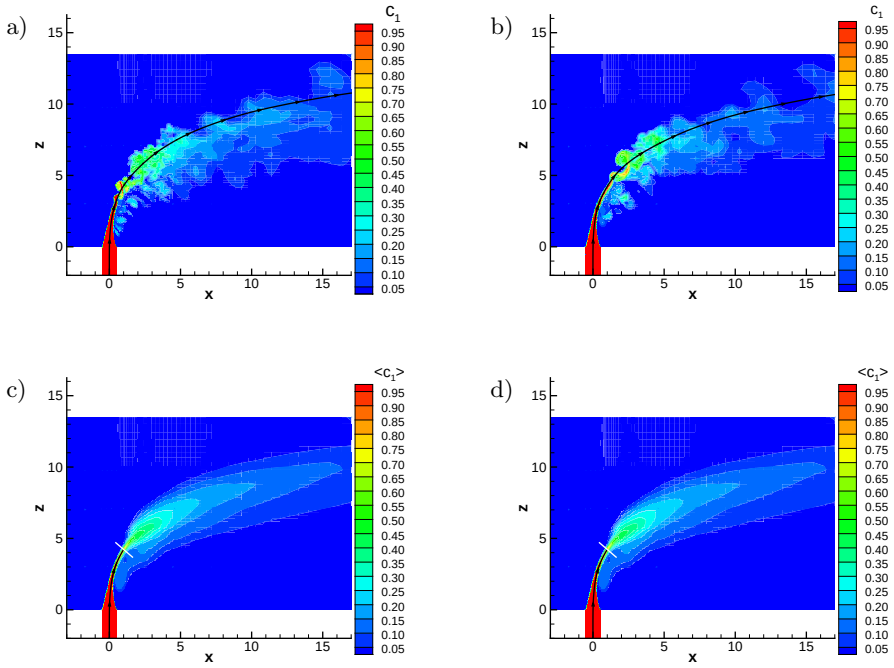

Fig. 6. Location of the transition point - visualized by the scalar concentration. a) Instantaneous scalar concentration at plane $y = 0$ ($Re = 650$), b) instantaneous scalar concentration at plane $y = 0$ ($Re = 325$), c) averaged scalar concentration at plane $y = 0$ ($Re = 650$) and the location of transition, d) averaged scalar concentration at plane $y = 0$ ($Re = 325$) and the location of transition.

9 Location of the transition

It can be deduced from the spatial distribution of the plotted variables in Figs. 4 and 5, that the transition occurs at different heights (i.e. different z-values) for the upstream and downstream parts of the jet. In order to seek for a universal measure to define the location of transition, the concentration distribution in the symmetry plane $y = 0$ together with the central streamline (0.;0.;0.) of the averaged flowfield are plotted in Fig.6. Now, from Fig. 6a and 6b the location of transition in the symmetry plane ($y = 0$) is easy to deduce. However, although not shown here explicitly, the transition location changes with time. Therefore, it was decided that the averaged scalar field presents a better measure for the transition point. For this reason the averaged scalar distribution along the streamline trajectory is considered. As it can be seen from Figs. 5c and 5d, the transition is characterised by a sudden enlargement of the scalar area along the streamline. This area is marked by the white "terminating" line for the streamline in Figs. 6c and 6d.

From Fig. 6 it becomes evident that the Reynolds number has a clear influence on the location of transition: transition occurs earlier in the case of higher Reynolds number. For $Re = 325$ the transition at the streamline trajectory occurs at $s/D = 4.41$ and for $Re = 650$ - at $s/D = 3.49$, or in other words, the transition occurs approximately one diameter earlier for the higher Reynolds number. Here, "s" is the path along the streamline starting from the point (0.;0.;0.).

10 Conclusions

Direct Numerical Simulation has been used to study the vortex structures of the jet in crossflow. The simultaneous computation and averaging of all important flow variables and scalar concentrations allows a detailed and concurrent analysis of the turbulent flow structures and the occurrence of transition.

A local grid refinement technique with a factor 3 : 1 allows an optimal distribution of the grid nodes of the block-structured grid within the computational domain. This contributes considerably to the efficiency of the numerical investigation and to the overall reduction of computational costs.

The use of a complex curvilinear grid and complex domain shape for the jet in crossflow requires a large number of processors optimising at the same time the distribution of the control volumes over the processors. The optimisation process applied here in a separate preprocessing step takes into account the histogram of the distribution of the number of control volumes per block, the number of control volumes in the largest blocks and the parallel efficiency, which in turn depends on the number of processors. For the present DNS the optimum distribution of control volumes per processor was found when using 31 or 32 processors, allowing parallel efficiency of 91% to be achieved on the XC HP 4000 high performance computer.

The Reynolds number has been found to be an important factor for the location of the transition region. At the same time its influence on the trajectory streamline of the flow is small.

Acknowledgements

The simulations were performed on the national super computer HP XC4000 at the High Performance Computing Center Stuttgart (HLRS) under the grant with acronym "$DNS - jet$".

References

1. J. A. Denev, J. Fröhlich, and H. Bockhorn. Direct numerical simulation of mixing and chemical reactions in a round jet into a crossflow. In W. E. Nagel, W. Jaeger,

and M. Resch, editors, *High Performance Computing in Science and Engineering 06, Transactions of the High Performance Computing Center Stuttgart*, pages 237–251. Springer - Heidelberg - New York, 2006.
2. Y. Dubief and F. Delcayre. On coherent-vortex identification in turbulence. *J. Turbulence*, 1(11), 2000.
3. T.F. Fric and A. Roshko. Vortical structure in the wake of a transverse jet. *J. Fluid Mech.*, 279:1–47, 1994.
4. B. A. Haven and M. Kurosaka. Kidney and anti-kidney vortices in crossflow jets. *J. Fluid Mech*, 352:27–64, 1997.
5. C. Hinterberger. *Dreidimensionale und tiefengemittelte Large–Eddy–Simulation von Flachwasserströmungen*. PhD thesis, Institute for Hydromechanics, University of Karlsruhe, http://www.uvka.de/univerlag/volltexte/2004/25/, 2004.
6. T. T. Lim, T. H. New, and S. C. Luo. On the development of large-scale structure of a jet normal to a cross flow. *Phys. Fluids*, 13(3):770–775, March 2001.
7. R.J. Margason. 50 years of jet in cross flow research. In *Computational and experimental assessment of jets in crossflow*, pages 1.1–1.41, AGARD-CP-534, 1993.
8. S. Narayanan, P. Barooah, and J.M. Cohen. Experimental study of the coherent structure dynamics and control of an isolated jet in crossflow. AIAA Paper 2002-0272, 2002.
9. L.L. Yuan and R. L. Street. Trajectory and entrainment of a round jet in crossflow. *Phys. Fluids*, 10(9):2323–2335, 1998.